

Microbial population and functional dynamics associated with surface potential and carbon metabolism

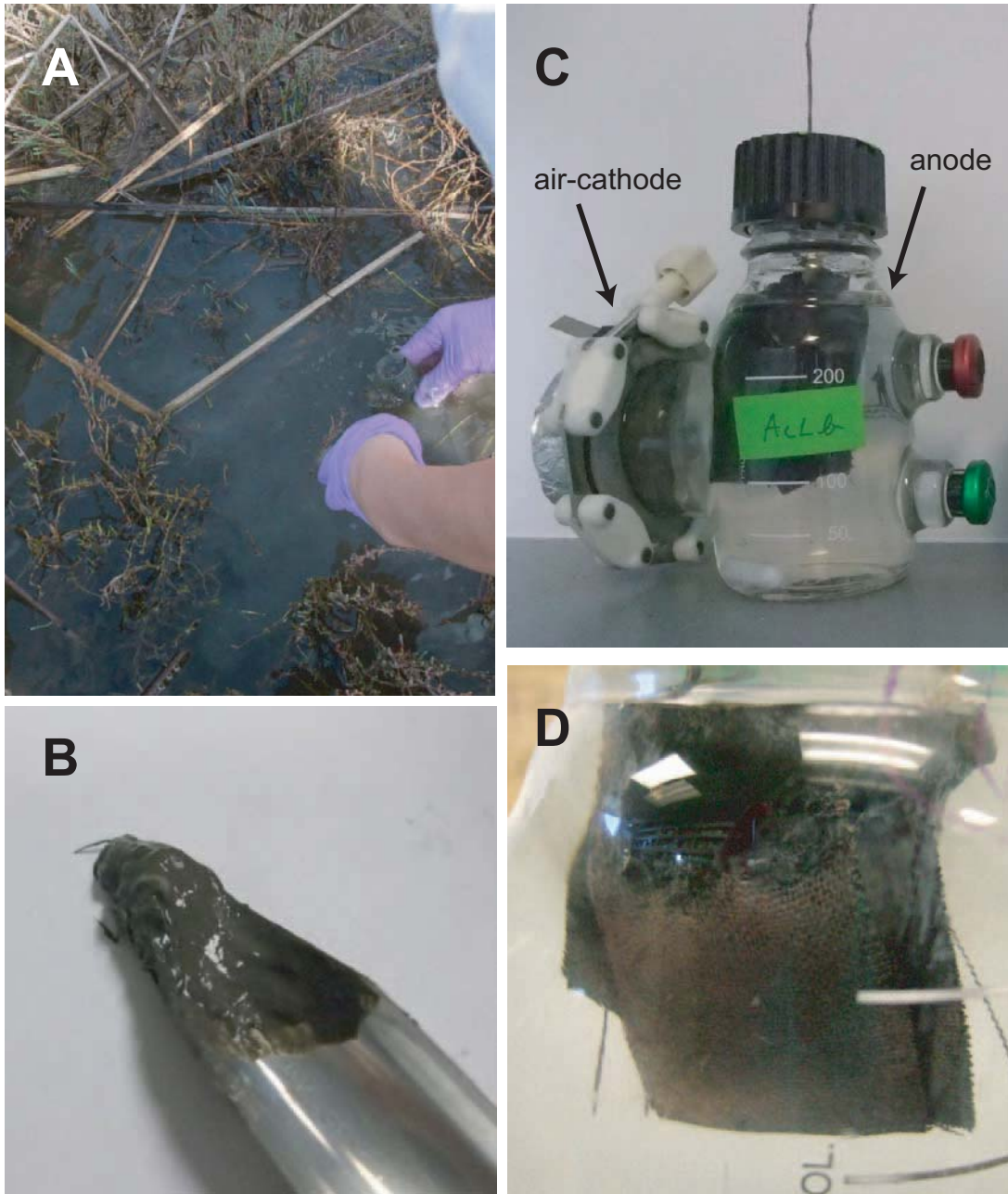
Shun'ichi Ishii*, Shino Suzuki*, Trina M. Norden-Krichmar, Tony Phan, Greg Wanger, Kenneth H. Nealson, Yuji Sekiguchi, Yuri A. Gorby, Orianna Bretschger

* Corresponding authors
SI, E-mail: sishii@jcvj.org; Tel: +1-858-200-1841; Fax: +1-858-200-1801
SS, E-mail: shishii@jcvj.org; Tel: +1-858-200-1858; Fax: +1-858-200-1801

SUPPLEMENTARY INFORMATION

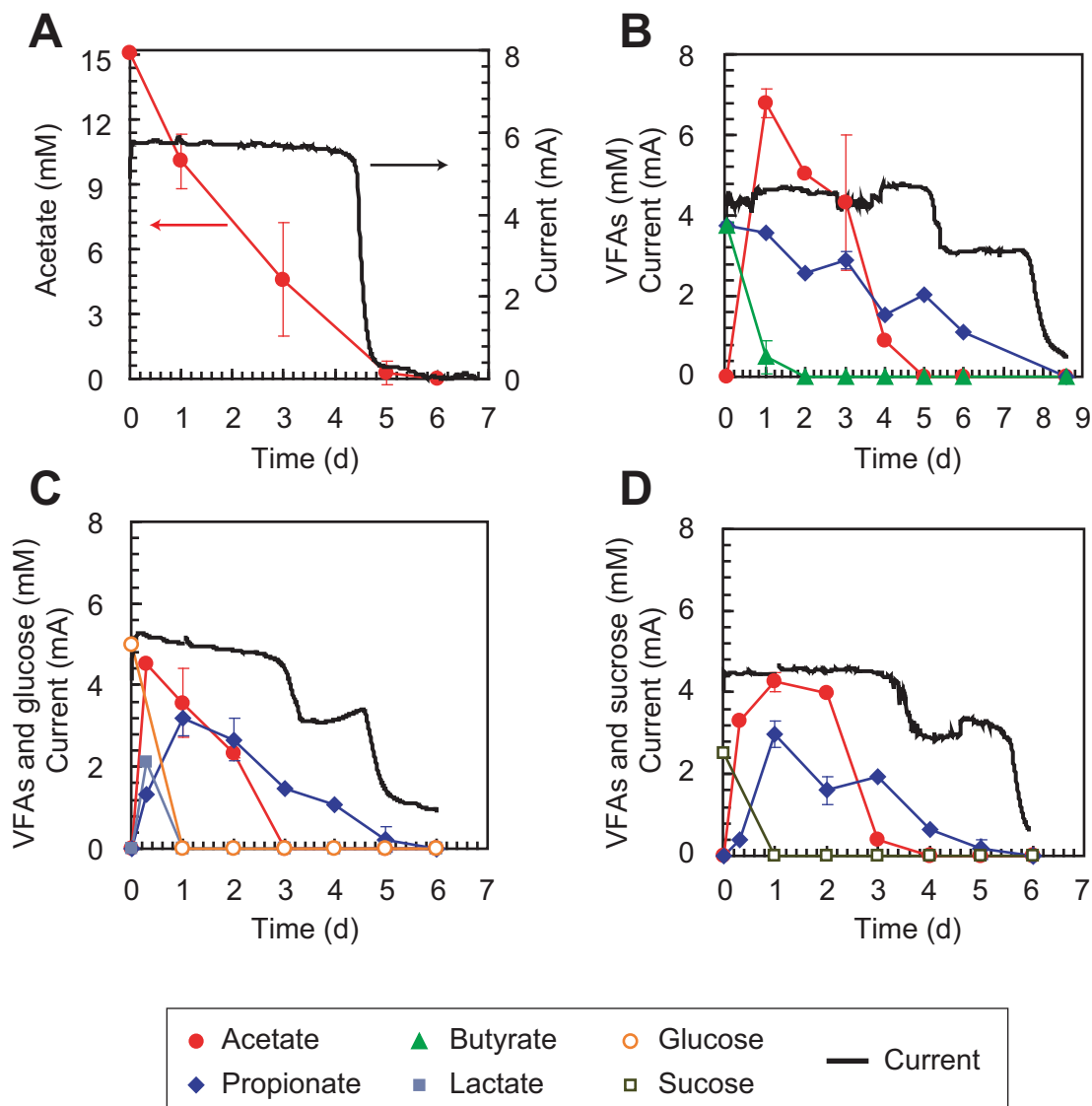
Table of Contents

SUPPLEMENTARY FIGURES.....	2
SUPPLEMENTARY TABLES	13
SUPPLEMENTARY METHODS	19
Medium composition	19
HPLC analyses.....	19
Scanning electron microscopy (SEM)	19
SUPPLEMENTARY DISCUSSION.....	20
Microbial metabolic functions in AC-MFC	20
Microbial metabolic functions in BP-MFC.....	21
Sugar metabolism-related strains in EET-active communities	22
<i>Geobacter</i> phylotype trends in EET-active communities	23
SUPPLEMENTARY REFERENCES.....	24



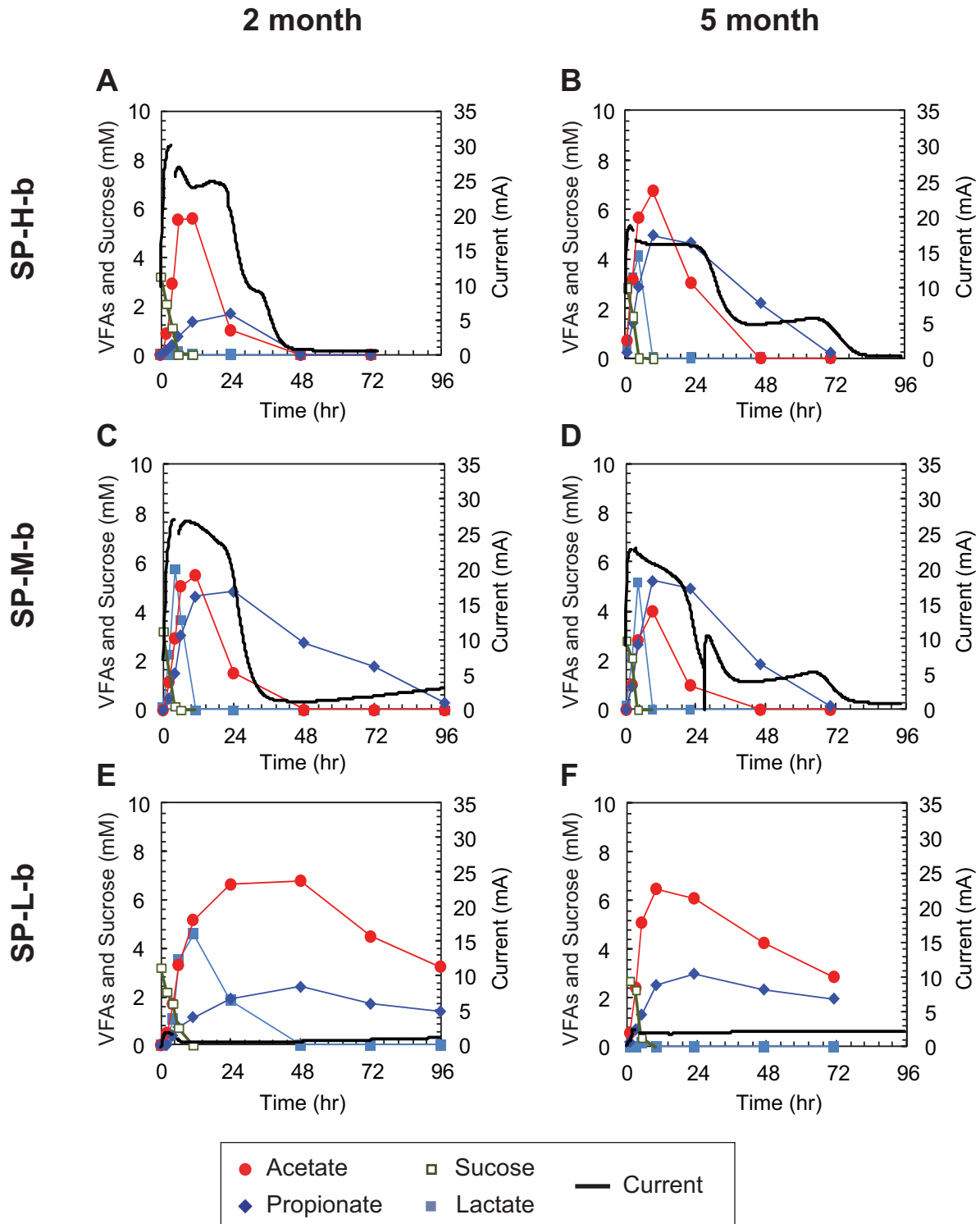
Supplementary Fig. S1. Microbial fuel cell (MFC) used in this study.

Sampling of San Elijo lagoon sediments, San Diego (A). Inoculum source of slurry from the lagoon sediment (B). The air-cathode MFC used in this study, where the anode and the air-cathode were connected with a resistor (C). The anode biofilm with pink color in a glucose-fed MFC after 3 months of enrichment (D).



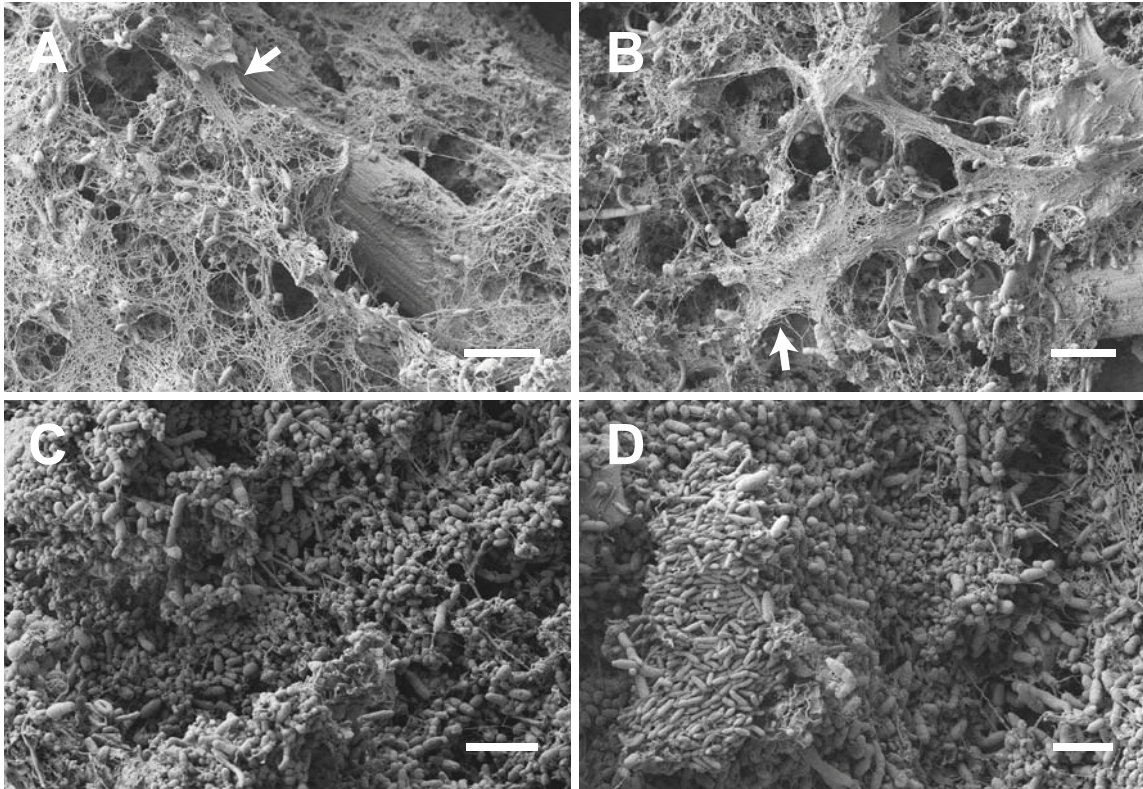
Supplementary Fig. S2. Exemplary current generation and substrate consumption rates in second set of MFCs.

Typical batch cycle of reactor ‘b’ of AC-MFCs (A), BP-MFCs (B), GL-MFCs (C), and SU-MFCs (D) after the 3-month enrichment process. The black line indicates electric current (mA) with 22 Ohm external resistance.



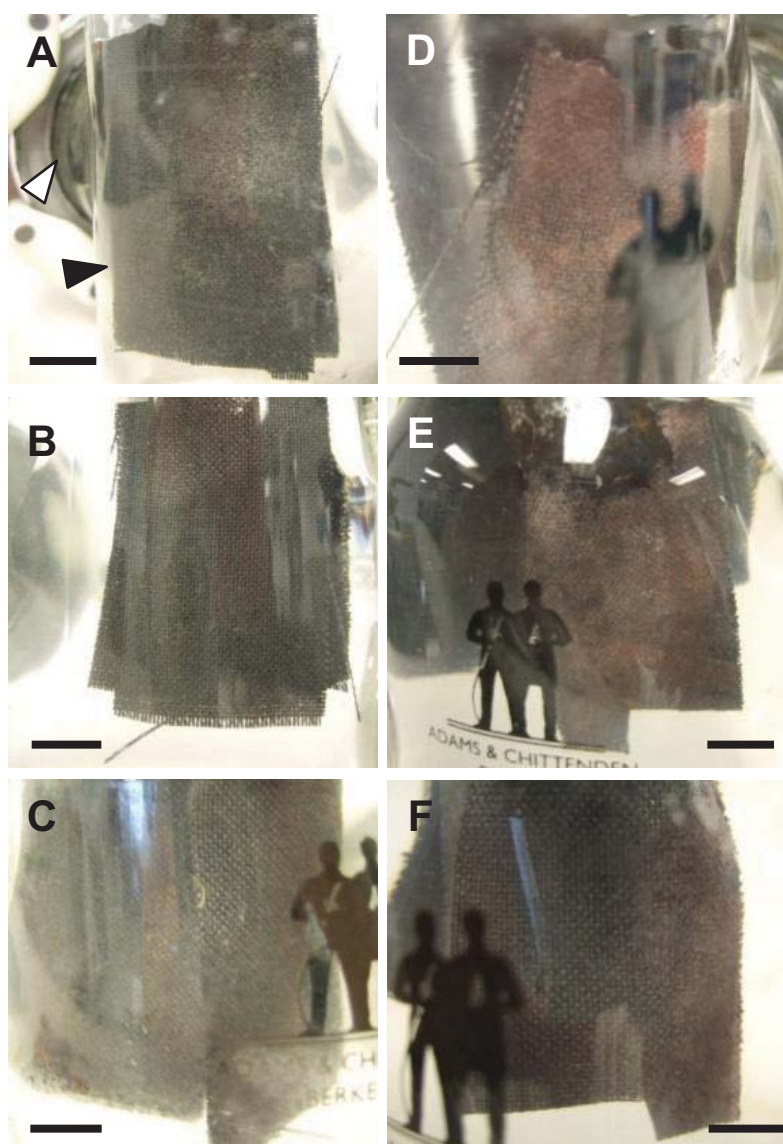
Supplementary Fig. S3. Exemplary current generation and substrate consumption rates in second set of SP reactors.

Typical batch cycle of reactor ‘b’ under SP-H (A, B), SP-M (C, D), and SP-L (E, F) operation after the 2-month (A, C, E) and 5-month (B, D, F) enrichment process. The black line indicates electric current (mA) under anode potential controlled operations.



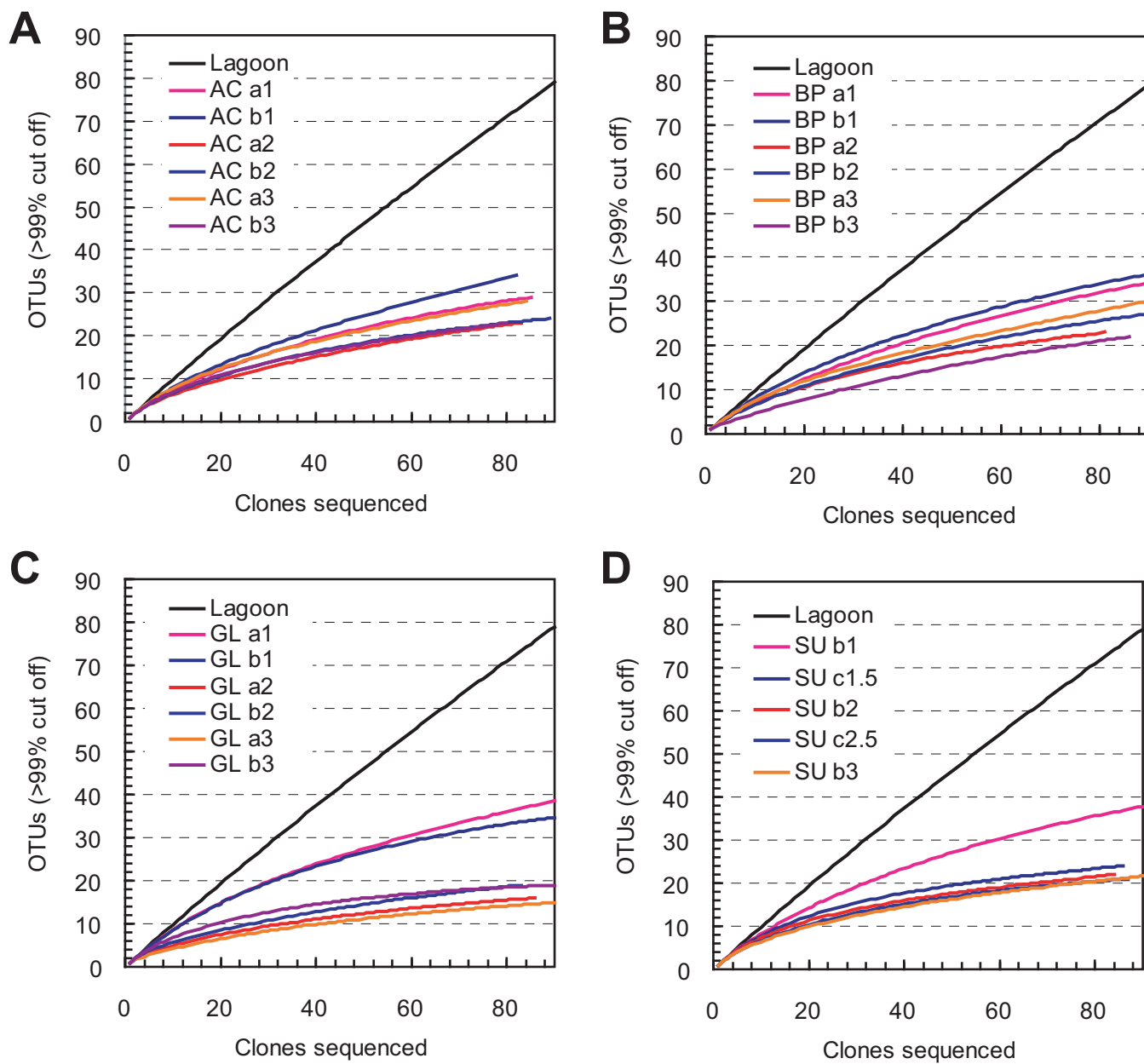
Supplementary Fig. S4. FE-SEM images for anode biofilms adhering onto carbon cloth electrodes.

Anode samples were collected from AC-MFC (A), BP-MFC (B), GL-MFC (C), and SU-MFC (D) after 3-month enrichment process. Arrows in panels A and B indicate filamentous structures in the biofilm. Bars = 5 μm .



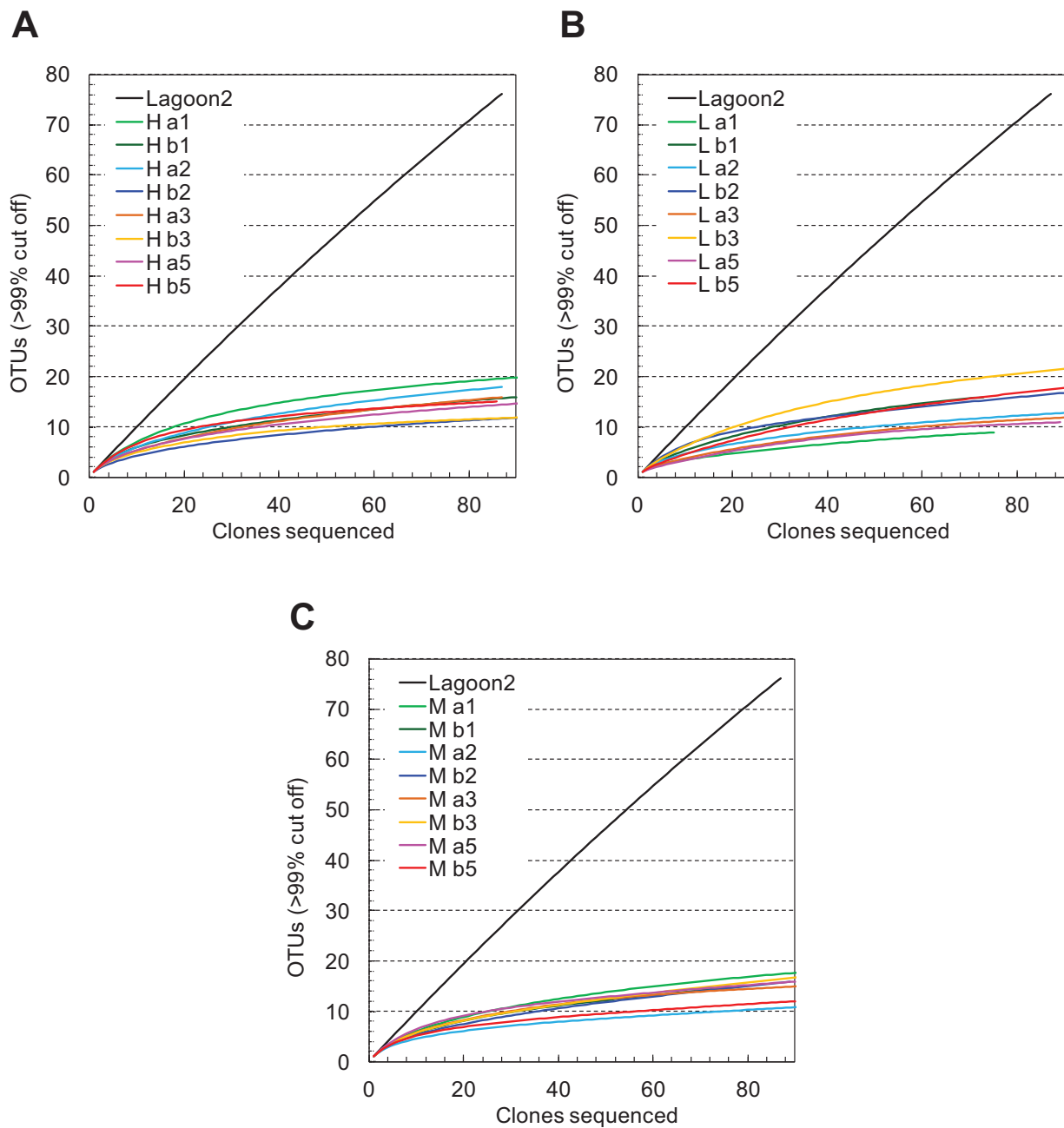
Supplementary Fig. S5. Electricity-generating biofilms during the enrichment process under controlling anode potentials.

Anodic biofilms after 2-month (A-C) and 5-month (D-F) of SP operation controlling the anode potentials to +100 mV vs SHE (A for H-a2, D for H-a5), -50 mV vs SHE (B for M-a2, E for M-a5), and -200 mV vs SHE (C for L-a2, F for L-a5). Filled arrowhead indicates carbon cloth anode, Open arrowhead indicates the air-cathode located on the side port of the reactor. Bars are 1 cm.



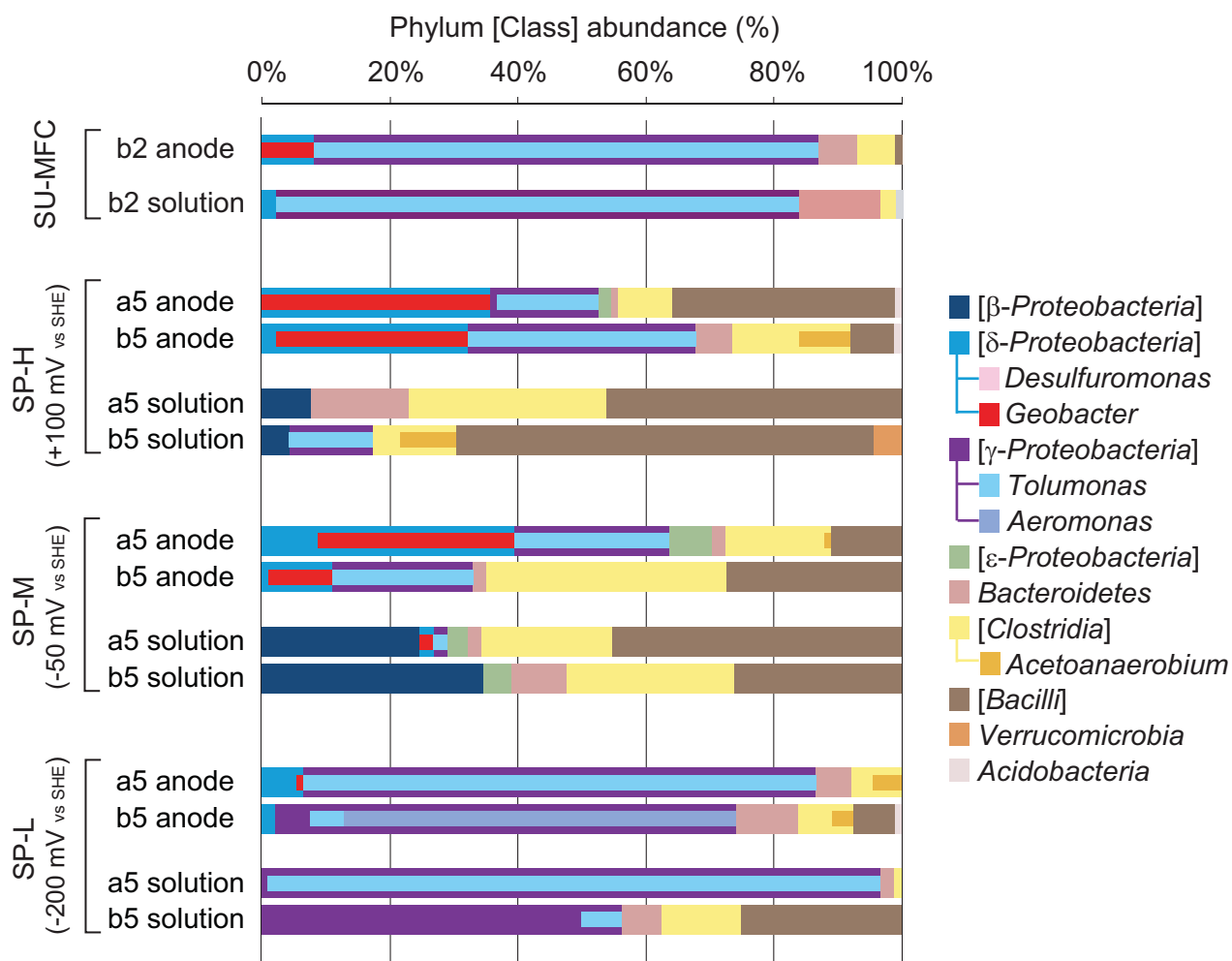
Supplementary Fig. S6. Rarefaction curves for the different phylotypes obtained from 16S rRNA gene clone libraries.

The anode samples in duplicate MFCs (a and b) fed with acetate (A), mixture of butyrate and propionate (B), glucose (C), and sucrose (D) were collected at 1 month, 2 months, and 3 months of enrichment.



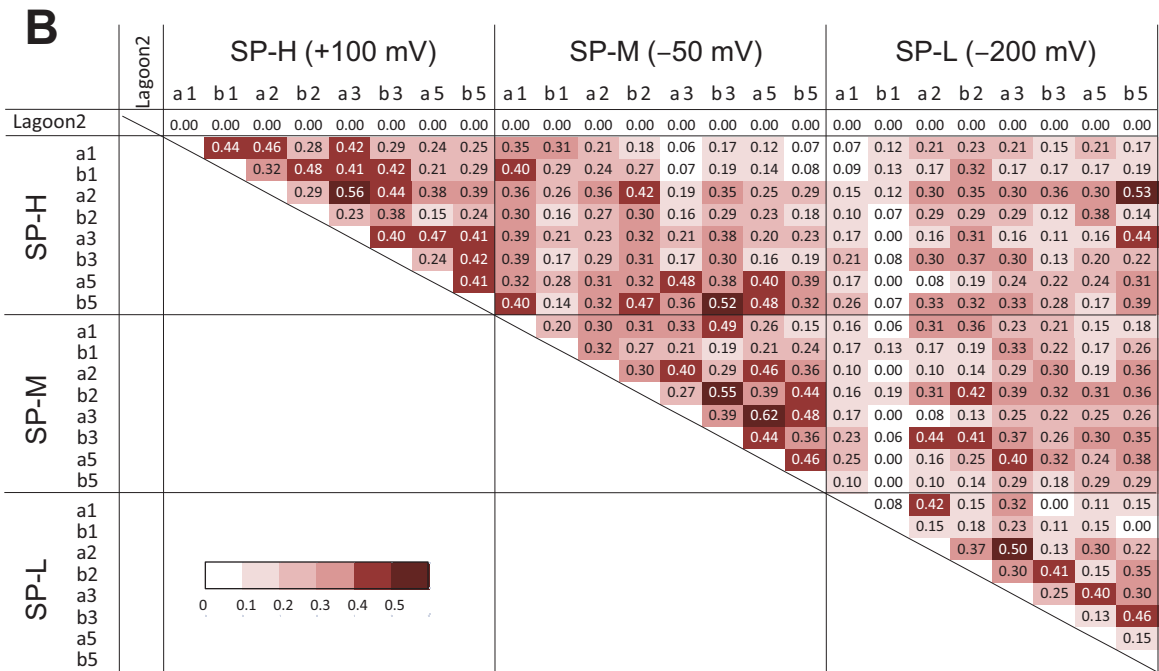
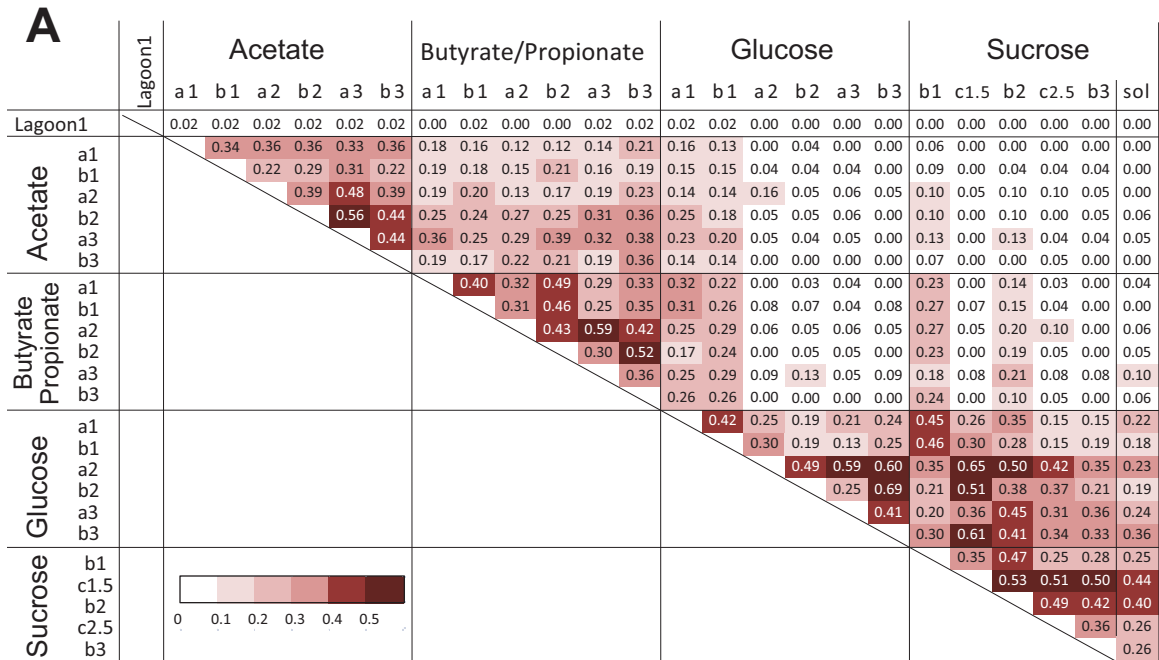
Supplementary Fig. S7. Rarefaction curves for the different phylotypes obtained from 16S rRNA gene clone libraries from three SP operations.

The anode samples in duplicate SP reactors (a and b) fed with sucrose, and controlled under +100 mV vs SHE (A), -50 mV vs SHE (B), and -200 mV vs SHE (C), were collected at 1 month, 2 months, 3 months, and 5 months of enrichment.



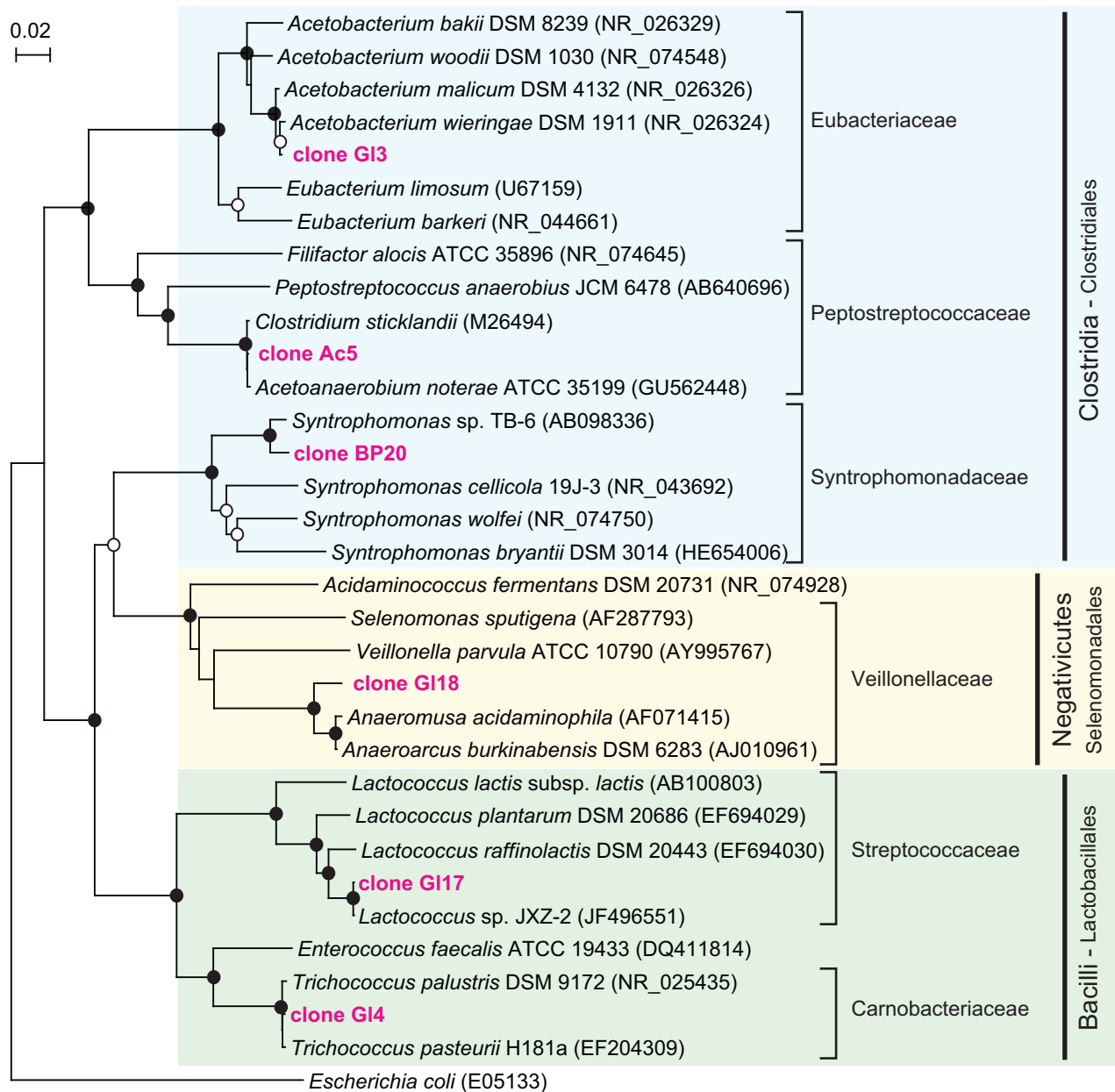
Supplementary Fig. S8. Phylum-Class level taxonomic distribution of 16S rRNA community profiles between anode biofilm and anolyte suspension.

The taxonomic profiles were compared between anode biofilm (anode) and anolyte suspension (solution) for the SU-MFC-b at 2 months of enrichment, and for the three different SP operations (SP-H, SP-M, and SP-L) at 5 months of enrichment. Phylum *Proteobacteria* and *Firmicutes* are divided into class level taxonomies. Five dominant genera in the communities are shown in inner bars.



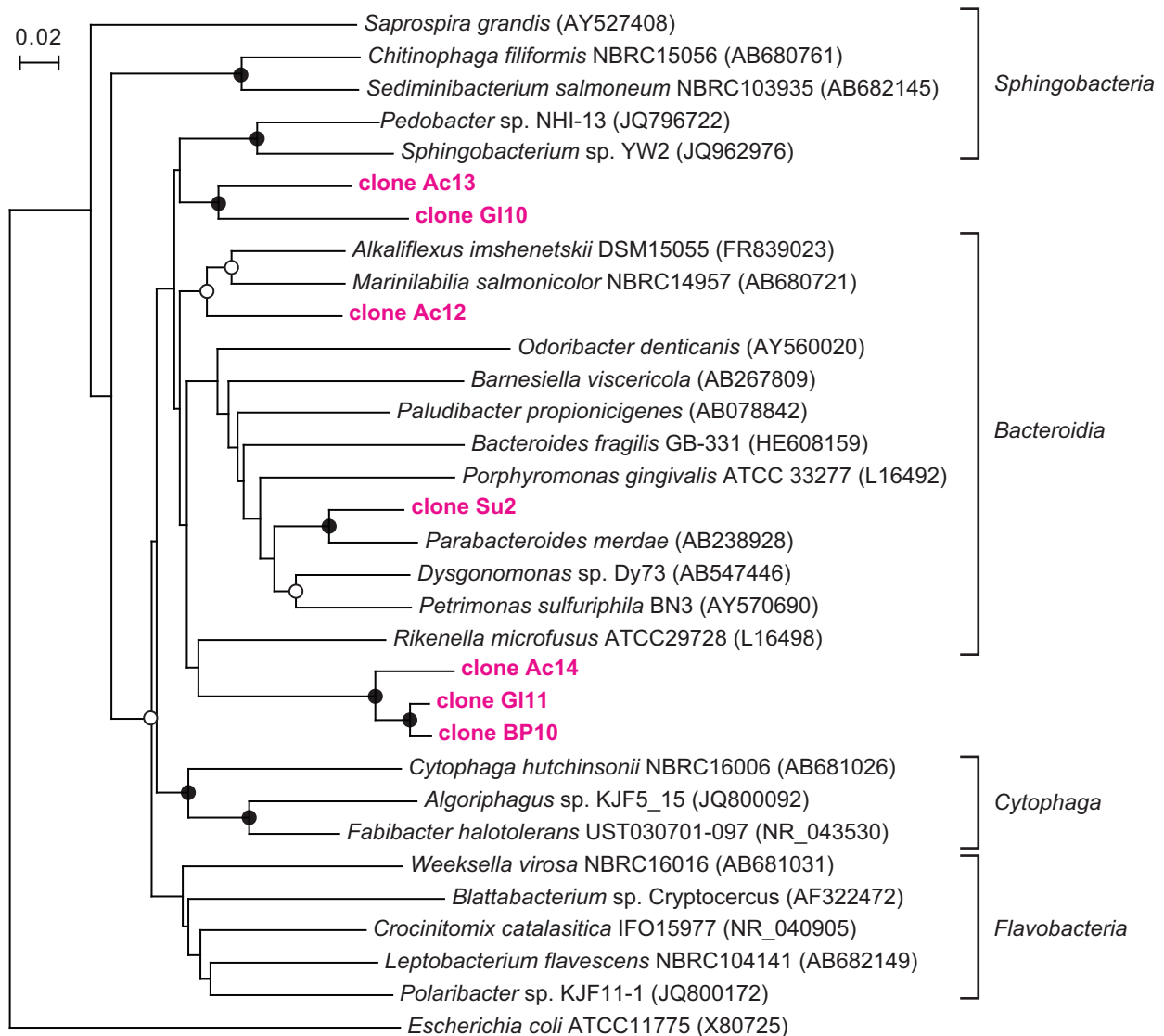
Supplementary Fig. S9. Sorensen similarities comparing the bacterial communities based on O.T.U. (99% cutoff).

Anodic community similarity comparison among four different substrates-fed MFCs (A) and among three different set-potential operations fed with sucrose (B).



Supplementary Fig. S10. A neighbor-joining phylogenetic tree showing positions of major phylotypes representing anodic microbial populations for phylum *Firmicutes*.

Branch points supported with bootstrap values (100 trials) of >90% are indicated with closed circles, while those between 70% and 90% are indicated with open circles. Accession numbers of reference sequences are indicated in parentheses.



Supplementary Fig. S11. A neighbor-joining phylogenetic tree showing positions of major phylotypes representing anodic microbial populations for phylum *Bacteroidetes*.

Branch points supported with bootstrap values (100 trials) of >90% are indicated with closed circles, while those between 70% and 90% are indicated with open circles. Accession numbers of reference sequences are indicated in parentheses.

Supplementary Table S1. Alpha diversity statistics of microbial communities from MFC anode biofilms fed with four different substrates and from lagoon sediment.

Substrate	Lagoon 1	AC-MFC Acetate			BP-MFC Butyrate / Propionate								
		a-1	b-1	a-2	a-3	b-1	a-2	b-2	a-3	b-3			
Reactor ID - Month													
Total clones sequenced	90	85	82	83	89	84	80	126	89	81	89	94	86
Number of OTU (99% cutoff)	79	27	32	23	23	27	23	40	36	22	25	29	21
Chao1 Richness ^a	439 ±88	41 ±8	87 ±25	37 ±9	33 ±7	43 ±9	59 ±21	68 ±13	59 ±11	33 ±8	37 ±7	129 ±46	38 ±10
Shannon's Index	4.3	2.49	2.81	2.42	2.52	2.75	2.59	2.91	3.17	2.49	2.51	2.71	1.77
Simpson Index (1 - D)	0.98	0.82	0.88	0.85	0.86	0.9	0.88	0.88	0.94	0.86	0.85	0.9	0.62
Substrate		GL-MFC Glucose			SU-MFC Sucrose								
Reactor ID - Month		a-1	b-1	a-2	b-2	a-3	b-3	b-1	c-1.5	b-2	c-2.5	b-3	b-2 sol ^b
Total clones sequenced		92	92	86	83	91	90	91	86	84	87	94	86
Number of OTU (99% cutoff)		34	33	14	19	13	16	37	20	18	19	20	13
Chao1 Richness ^a		84 ±23	44 ±6	32 ±15	44 ±16	31 ±15	18 ±2	57 ±10	28 ±7	66 ±30	24 ±4	33 ±8	22 ±8
Shannon's Index		3.06	3.16	1.77	2.19	1.48	2.22	3.2	2.61	2.18	2.03	2.18	1.64
Simpson Index (1 - D)		0.93	0.94	0.71	0.83	0.6	0.85	0.93	0.9	0.83	0.73	0.82	0.68

^a Value ± SD.

^b Microbial community of anolyte solution (sol) was analyzed for SU-MFC-b at 2 month.

Supplementary Table S2. Alpha diversity statistics of microbial communities from anode biofilms under three different set-potential operations fed with sucrose.

Anode potential (vs SHE) Reactor ID - Month	Lagoon 2	SP-H +100 mV									
		a-1	b-1	a-2	b-2	a-3	b-3	a-5	b-5	a-sol ^a	b-sol ^a
Total clones sequenced	88	94	91	88	94	88	94	95	87	13	22
Number of OTU (99% cutoff)	77	18	14	17	11	15	10	15	14	4	6
Chao1 Richness ^b	326 ±63	24 ±5	18 ±4	42 ±19	13 ±2	24 ±8	15 ±5	24 ±8	18 ±4	5 ±1	12 ±7
Shannon's Index	4.30	2.37	2.05	2.17	1.28	1.96	1.47	1.99	2.11	1.20	1.09
Simpson Index (1 - D)	0.99	0.87	0.83	0.83	0.55	0.79	0.68	0.80	0.82	0.66	0.51
Anode potential (mV vs SHE) Reactor ID - Month		SP-M -50 mV									
		a-1	b-1	a-2	b-2	a-3	b-3	a-5	b-5	a-sol ^a	b-sol ^a
Total clones sequenced		95	79	94	90	93	93	91	91	93	23
Number of OTU (99% cutoff)		16	14	11	16	14	17	15	11	16	7
Chao1 Richness ^b		28 ±10	39 ±19	21 ±10	52 ±26	22 ±8	58 ±28	24 ±8	24 ±12	57 ±28	13 ±7
Shannon's Index		2.08	1.82	1.66	2.00	2.07	2.13	2.19	1.74	1.82	1.59
Simpson Index (1 - D)		0.82	0.73	0.74	0.81	0.83	0.83	0.86	0.78	0.74	0.76
Anode potential (mV vs SHE) Reactor ID - Month		SP-L -200 mV									
		a-1	b-1	a-2	b-2	a-3	b-3	a-5	b-5	a-sol ^a	b-sol ^a
Total clones sequenced		76	74	96	93	93	95	90	93	88	16
Number of OTU (99% cutoff)		9	16	10	17	10	22	10	17	7	7
Chao1 Richness ^b		20 ±3	13 ±4	49 ±23	14 ±4	28 ±5	14 ±4	37 ±14	12 ±3	15 ±8	13 ±7
Shannon's Index		1.29	1.96	0.99	2.31	0.86	2.33	1.03	1.64	0.74	1.72
Simpson Index (1 - D)		0.63	0.75	0.40	0.87	0.33	0.81	0.40	0.61	0.35	0.79

^a Microbial community of anolyte solution (sol) was determined only on 5 month samples.

^b Value ± SD.

Table S3. continued.

Taxonomy Phylotype	Lagoon	Acetate				Butyrate / Propionate				Glucose				Sucrose				SUM	% match	Best matched sequence	Accession No.						
		a-1	b-1	a-2	b-2	a-3	b-3	a-1	b-1	a-2	b-2	a-3	b-3	a-1	b-1	a-2	b-2					a-3	b-3				
<i>Bacteroidetes</i>																											
Su1	-	-	-	-	-	-	-	-	-	-	2	2	-	-	1	3	2	-	-	1	11	93%	<i>Paludibacter propionicigenes</i>	AB078842			
Ac24	-	-	-	3	1	-	-	-	-	-	-	-	-	-	-	-	-	-	-	-	4	91%	<i>Paludibacter propionicigenes</i>	AB078842			
GLE10	-	-	-	-	-	-	-	-	-	-	-	3	-	-	-	-	-	-	-	-	3	96%	<i>Paludibacter propionicigenes</i>	AB078842			
Su2	-	-	-	1	-	-	-	1	1	-	1	2	2	3	-	5	3	14	1	3	38	100%	<i>Porphyromonadaceae</i> bacterium JN18_A107_G	DQ168658			
Ac25	-	-	-	3	-	4	-	-	-	-	1	-	-	-	-	-	-	-	-	-	8	99%	<i>Petrimonas sulfuriphila</i> strain BN3	AY570690			
Ac12	-	4	5	10	16	2	5	4	-	-	-	-	-	-	-	-	-	-	-	-	46	93%	<i>Sphingobacteriales</i> bacterium Kimo37	AB260041			
Ac23	-	-	-	-	-	1	1	-	-	-	-	-	-	-	-	-	-	-	-	-	2	92%	<i>Sphingobacteriales</i> bacterium Kimo37	AB260041			
Ac11	-	2	-	3	4	3	1	-	1	-	-	-	-	-	-	-	-	-	-	-	16	92%	<i>Rikenellaceae</i> bacterium JAM-BA0501	AB362265			
Ac10	-	2	2	-	2	1	-	1	-	-	-	-	-	-	-	-	-	-	-	-	9	94%	<i>Alkaliflexus imshenetskii</i> Z-7010	AJ784993			
GI20	-	-	-	-	-	-	-	-	-	-	-	-	1	1	1	-	1	-	-	2	2	82%	<i>Bacteroides intestinalis</i> JCM 13266	AB214329			
Su4	-	-	-	-	-	-	-	-	2	-	1	-	-	-	-	2	-	-	-	-	7	87%	<i>Cellulophaga tyrosinoxydans</i> EM41	EU443205			
GI22	-	-	-	-	-	-	-	-	-	-	-	-	1	-	1	-	-	2	-	-	4	86%	<i>Lutaonella thermophilus</i> CC-MHSW-2	EU287913			
Su8	-	-	-	-	-	-	-	-	-	-	-	-	-	-	1	-	1	-	-	-	2	87%	<i>Lutaonella thermophilus</i> CC-MHSW-2	EU287913			
GI21	-	-	-	-	-	-	-	-	-	-	-	-	2	-	2	-	-	-	-	-	6	90%	<i>Rikenellaceae</i> bacterium WN081	AB298736			
BP27	-	-	-	-	-	1	4	6	-	-	-	-	-	-	-	-	-	-	-	-	11	88%	<i>Cytophaga fermentans</i>	M58766			
BP26	-	-	-	-	-	-	4	1	-	-	-	-	-	-	-	-	-	-	-	-	5	88%	<i>Flexibacter canadensis</i> IFO 15130	AB078046			
BP25	-	-	-	-	-	1	-	-	2	-	-	-	-	-	-	-	-	-	-	-	3	89%	<i>Pedobacter daechungensis</i> Dae 13	AB267722			
Ac13	-	10	-	22	4	19	11	-	1	-	2	-	2	-	-	-	-	-	-	-	71	88%	<i>Riemerella anatipestifer</i> ATCC 11845	U10877			
BP10	-	-	-	-	1	15	3	9	4	10	1	6	2	-	-	3	-	1	-	-	55	88%	<i>Bacteroidetes</i> bacterium T4-KAD-str1	AJ575808			
Ac14	1	1	5	4	6	2	4	-	1	-	1	5	1	1	-	-	-	-	-	-	32	87%	<i>Bacteroidetes</i> bacterium clone WWP_SS3_G18	GU409275			
GI10	-	-	-	-	-	-	-	-	1	1	-	2	-	3	-	2	-	1	1	-	7	86%	<i>Sphingobacteriaceae</i> bacterium Gsoil	EU370954			
GI11	-	-	-	-	2	1	-	3	-	4	3	2	1	3	5	-	-	1	-	1	27	87%	<i>Bacteroidetes</i> bacterium T4-KAD-str1	AJ575808			
BP9	-	-	1	-	1	2	-	1	1	1	2	1	-	2	-	-	3	-	-	1	16	87%	<i>Bacteroidetes</i> bacterium T4-KAD-str1	AJ575808			
Ac15	-	2	3	-	-	1	-	-	-	-	-	-	-	-	-	-	-	-	-	-	6	84%	<i>Pedobacter</i> sp. DL5	FJ517612			
Su3	-	-	-	-	-	-	-	1	-	-	-	-	-	1	-	-	-	-	-	-	3	90%	<i>Flexibacter</i> sp. R2A36-4	EU787448			
BP7	-	-	1	1	-	-	-	1	-	-	-	-	-	-	-	-	-	-	-	-	3	99%	<i>Rikenellaceae</i> bacterium WN081	AB298736			
BP8	-	-	-	-	-	1	-	-	-	-	-	1	-	-	-	-	-	-	-	-	2	87%	<i>Pontibacter</i> sp. HMD3093	HM135524			
<i>Tenericutes - Mollicutes</i>																											
BP14	-	-	-	1	-	6	-	3	-	2	-	2	-	-	-	-	-	-	-	-	14	98%	<i>Acholeplasma polakii</i>	AF031479			
Ac22	-	-	-	1	2	2	3	-	-	-	-	-	-	-	-	-	-	-	-	-	8	92%	<i>Acholeplasma palmae</i>	L33734			
BP_P04	-	-	-	-	-	-	-	3	-	-	-	-	-	-	-	-	-	-	-	-	3	99%	<i>Acholeplasma</i> sp. DM-2009 strain Lorelei	FJ590762			
Other phyla and Unclassified																											
BP24	-	-	-	-	-	1	-	1	-	-	-	-	-	-	-	-	-	-	-	-	2	99%	<i>Spirochaeta</i> sp. Buddy	AF357916			
BP19	-	-	-	-	-	-	1	-	2	-	-	-	-	-	-	-	-	-	-	-	3	88%	<i>Clostridium putrefaciens</i>	AF127024			
Ac_I20	-	-	-	3	-	-	-	-	-	-	-	-	-	-	-	-	-	-	-	-	3	84%	<i>Dehalococcoides</i> sp. BH180-15	AJ431246			
Ac26	-	-	-	2	-	1	1	1	-	1	-	-	-	-	-	-	-	-	-	-	6	90%	<i>Bacteroidales</i> bacterium 33bM	GU129118			
GI_O13	-	-	-	-	-	-	-	-	-	-	-	-	-	3	-	-	-	-	-	-	3	85%	<i>Solobacterium moorei</i> F0204	GU470893			
BP23	-	-	-	-	-	1	-	-	1	-	-	-	-	-	-	-	-	-	-	-	2	84%	Unidentified eubacterium clone BSV19	AJ229184			
BP3	-	-	-	-	-	3	3	-	-	-	-	1	-	-	-	2	-	-	-	-	9	86%	<i>Erysipelothrix rhusiopathiae</i> B 470/87	EF050040			
Rare population ^b																											
	89	11	18	6	5	6	5	11	12	3	4	7	2	9	7	-	3	2	-	10	1	1	4	4	3	223	Unidentified
Total clones	90	85	82	83	89	84	80	126	89	81	89	94	86	92	92	86	83	91	90	91	86	84	87	94	86	2220	

^a Microbial community analysis of anolyte solution (sol) after batch was conducted at 2 month samples fed with sucrose.

^b Rare population included phylotypes which were shown in only one library with less than 2 clones.

Supplementary Table S4. All phylotypes (n>2) obtained from anode biofilms under three different set-potential operations.

Taxonomy Phylotype	Lagoon2	SP-H					SP-M					SP-L					SUM	% match	Best matched sequence	Accession No.									
		a-1	a-2	a-3	a-5	b-1	b-2	b-3	b-5	a-1	a-2	a-3	a-5	b-1	b-2	b-3					b-5	a-1	a-2	a-3	a-5	b-1	b-2	b-3	b-5
Proteobacteria - δ-Proteobacteria																													
G11	-	9	26	24	6	3	-	29	4	44	8	-	-	1	-	-	-	-	-	-	-	-	39	-	193	96	<i>Geobacter</i> sp. CdA-2	Y19190	
G12	-	-	-	-	-	17	13	3	-	-	-	-	-	-	-	-	-	1	-	2	-	-	1	-	37	97	<i>Geobacter</i> sp. Ply1	EF527233	
MEC_GeoH3	-	-	-	5	23	-	-	-	10	1	-	5	-	-	-	1	-	-	-	-	-	-	-	-	45	98	<i>Geobacter humireducens</i>	AY187306	
G115	-	-	-	-	-	-	-	-	-	-	-	18	19	-	-	7	9	-	-	-	4	-	-	-	57	95	<i>Geobacter chapelleii</i>	U41561	
MEC_GeoM2	-	-	-	-	-	-	-	-	-	-	25	25	7	-	-	-	-	-	-	-	-	-	-	-	57	99	<i>Geobacter bremensis</i>	JN795198	
Su6	-	-	-	-	-	-	-	-	11	-	-	-	-	-	-	-	-	-	-	-	-	-	-	11	99	<i>Geobacter</i> sp. OSK6	AB682759		
Ha4_I01	-	-	-	4	-	-	-	-	-	-	-	-	-	-	-	-	-	-	-	-	-	-	-	4	99	<i>Geobacter</i> sp. CLFeRB	DQ086800		
Su5	-	-	-	-	-	-	-	-	-	-	3	7	-	-	-	-	-	-	-	-	-	6	-	16	98	<i>Pelobacter propionicus</i> DSM 2379	CP000482		
Geo1	-	1	-	-	-	-	-	-	1	-	-	2	-	-	1	-	4	2	3	-	-	-	-	14	96	<i>Geobacter metallireducens</i> GS-15	CP000148		
Ac3	-	-	-	-	-	-	-	-	-	-	-	-	-	-	-	10	-	-	-	-	-	-	-	10	98	<i>Geobacter sulfurreducens</i> KN400	CP002031		
Geo2	-	-	-	-	-	-	-	-	-	-	-	-	-	6	-	-	-	-	-	-	-	-	-	6	97	<i>Geobacter metallireducens</i> GS-15	CP000148		
Ha2_G01	-	3	-	-	-	-	-	2	-	1	-	1	-	1	-	1	-	-	-	-	-	1	2	12	99	<i>Desulfovibrio desulfuricans</i> SRB-22	FJ873799		
Proteobacteria - γ-Proteobacteria																													
Tol5	-	1	5	3	3	24	61	44	31	20	39	5	22	38	18	23	19	26	74	76	69	-	23	-	629	99	<i>Tolomonas</i> sp. OCF	GU370947	
MEC_TOL2	-	2	3	5	10	-	-	-	-	-	-	-	-	-	-	-	-	-	-	1	-	-	-	21	96	<i>Tolomonas auensis</i> DSM 9187	CP001616		
G113	-	18	20	1	1	7	-	-	-	-	-	-	-	1	-	-	-	-	-	-	-	-	10	4	119	97	<i>Aeromonas sharmana</i> GPTSA-6	DQ013306	
G112	-	13	12	4	-	-	-	-	-	-	-	-	-	-	-	-	-	-	-	-	-	-	5	34	98	<i>Aeromonas sharmana</i> CB-8	JF496528		
MEC_AER3	-	-	-	-	-	18	-	-	-	-	-	-	-	11	1	-	-	-	-	-	-	1	-	31	100	<i>Aeromonas allosaccharophila</i> B021	JN644057		
Hb1_A01	-	-	-	-	-	3	-	-	-	-	-	-	-	-	-	-	-	-	-	-	-	-	-	3	98	<i>Aeromonas sharmana</i> CB-8	JF496528		
MEC_AER4	-	22	1	-	-	-	-	-	-	-	-	-	-	-	-	-	-	-	-	-	-	1	-	24	100	<i>Aeromonas media</i> E2P37	JF920519		
Proteobacteria - ϵ-Proteobacteria																													
Ma3_I21	-	-	-	2	-	-	-	-	1	-	4	6	-	-	-	-	1	-	-	-	-	-	-	14	98	<i>Sulfurospirillum deleyianum</i> DSM 6946	CP001816		
Hb1_K13	-	-	-	-	2	1	-	-	-	-	-	-	-	-	-	-	-	-	-	-	-	-	-	3	98	<i>Campylobacter</i> sp. DSM806	AF144694		
Lagoon3_C12	3	-	-	-	-	-	-	-	-	-	-	-	-	-	-	-	-	-	-	-	-	-	-	3	98	<i>Sulfuricurvum kujense</i> K-2	AB080643		
Firmicutes - Bacilli																													
G117	-	-	4	31	33	-	-	6	6	8	9	21	10	2	28	26	25	-	-	1	-	-	7	4	6	227	100	<i>Lactococcus</i> sp. JXZ-2	JF496551
G14	-	-	-	-	-	-	-	-	-	-	-	-	-	6	-	-	-	38	2	1	-	34	-	81	99	<i>Trichococcus patagoniensis</i> PMagG1	NR_041841		
Firmicutes - Clostridia																													
La3_B21	-	-	-	-	-	-	-	-	-	-	-	-	-	-	-	-	-	-	-	-	-	-	5	100	<i>Clostridium</i> sp. P2	AY949856			
G113	-	9	1	3	-	1	2	4	7	3	-	1	6	11	2	-	2	3	3	4	1	25	-	91	98	<i>Acetobacterium submarinus</i>	AY485791		
Ma1_I16	-	-	-	-	-	-	-	-	2	-	1	-	-	-	-	-	-	-	-	-	-	-	-	3	99	<i>Anaerofilum agile</i>	X98011		
Firmicutes - others																													
Hb2_E04	-	-	-	-	-	2	-	-	-	-	-	-	-	-	-	-	1	-	3	-	-	-	-	6	92	<i>Phascolarctobacterium</i> sp. YIT 12068	AB490812		
Ma1_E18	-	-	-	-	-	-	-	-	2	-	-	-	-	-	1	-	-	1	-	-	-	1	-	5	92	<i>Acidaminococcus</i> sp. BV3L6	JN809763		
Hb1_O19	-	-	1	-	-	1	-	-	-	-	-	-	-	-	-	-	-	-	-	-	-	-	1	3	90	<i>Acidaminococcus intestini</i> ADV 255.99	NR_041894		
Ma3_I07	-	-	-	1	-	-	-	1	-	2	1	-	1	-	1	-	-	-	-	-	-	-	-	7	94	<i>Acidaminococcus fermentans</i> DSM20731	CP01859		
G118	-	-	6	7	-	-	-	8	-	5	3	10	-	20	13	28	-	-	-	-	-	7	1	108	99	<i>Anaerococcus burkinensis</i> DSM 6283	NR_025298		
Ha2_K19	-	2	2	-	-	-	-	-	-	-	-	-	-	-	-	-	-	-	-	-	-	-	-	4	99	<i>Sporomusa silvacetica</i>	Y09976		
Ma4_P11	-	-	-	-	-	-	-	-	2	-	-	-	-	-	-	-	-	-	-	-	-	2	-	4	99	<i>Anaerococcus burkinensis</i> DSM 6283	NR_025298		
La3_L09	-	-	1	-	-	-	-	-	1	-	-	-	1	1	-	1	-	-	1	-	-	2	7	15	95	<i>Veillonellaceae</i> bacterium 6-15	AB603498		
Mb4_B08	-	-	-	-	-	-	-	-	1	-	-	-	-	4	-	-	-	-	-	-	-	-	-	5	91	<i>Clostridium</i> sp. SW001	HM755724		
Mb2_F08	-	-	-	-	-	-	-	-	-	-	-	-	1	-	-	-	-	-	-	-	-	1	1	3	92	<i>Veillonellaceae</i> bacterium 6-15	AB603498		
Bacteroidetes																													
Su2	-	7	3	-	-	11	8	3	4	6	-	-	-	-	4	1	-	-	6	1	3	11	4	3	75	99	<i>Parabacteroides</i> sp. Lind7H	HQ020488	
La3_D17	-	-	-	-	-	-	-	-	-	-	1	-	-	-	-	-	-	-	-	-	-	-	2	3	94	<i>Proteiniphilum acetatigenes</i> TB107	AY742226		
La3_N05	-	-	-	-	-	-	-	-	-	-	-	-	-	-	-	-	-	-	-	-	-	1	1	2	99	<i>Petrimonas sulfuriphila</i> BN3	AY570690		
Lb2_I24	-	1	-	-	-	-	-	-	-	-	-	-	-	-	-	-	5	2	-	-	-	-	-	8	99	<i>Bacteroides</i> sp. 253c	AY082449		
BP10	-	1	-	-	-	-	-	-	-	-	-	-	1	-	-	-	-	-	-	-	-	2	-	4	84	<i>Cytophaga fermentans</i> NBRC 15936	AB517712		
G111	-	-	-	-	-	-	-	-	-	-	-	-	-	-	-	-	-	-	-	-	-	2	8	3	13	83	<i>Cytophaga fermentans</i> NBRC 15936	AB517712	
La1_I20	-	-	-	-	-	-	-	-	-	-	-	-	-	-	-	-	-	-	-	-	3	1	-	4	83	<i>Cytophaga fermentans</i> NBRC 15936	AB517712		
La1_G16	-	-	-	-	-	-	-	-	-	-	-	-	-	-	-	-	-	-	-	-	7	-	-	7	98	<i>Rikenellaceae</i> bacterium WN081	AB298736		
La4_A15	-	-	1	-	-	-	-	-	-	-	-	-	2	-	-	-	-	-	-	-	-	-	4	5	90	<i>Paludibacter propionigenes</i> WB4	CP002345		
Hb4_O16	-	-	-	-	-	-	-	1	-	-	-	-	-	-	-	-	-	-	-	-	-	1	1	3	84	<i>Ornithobacterium rhinotracheale</i>	CP003283		
G110	-	-	1	-	1	-	2	-	-	3	3	1	3	1	1	2	-	-	3	2	-	-	5	2	30	85	<i>Bacteroidetes</i> bacterium 4F6B	AB623230	
La3_B11	-	-	-	-	-	-	-	-	-	-	-	-	1	-	-	-	-	-	1	-	-	1	1	5	90	<i>Porphyromonadaceae</i> bacterium C941	JF803519		
Ha1_D22	-	4	3	1	-	2	1	1	-	3	1	-	-	-	-	-	-	-	-	-	-	-	-	16	95	<i>Bacteroidetes</i> bacterium RL-C	AB611036		
Other Taxa																													
Ha2_K05	-	-	1	-	-	-	-	-	-	-	-	-	-	-	-	-	-	-	-	-	-	-	1	1	3	100	<i>Brevundimonas diminuta</i> EC21X	KC128938	
Mb3_M22	-	-	-	-	-	-	-	-	-	-	-	-	-	-	1	3	-	-	-	-	-	-	-	4	88	<i>Dehalobacter</i> sp. E1	AY766465		
Mb3_K06	-	-	-	-	-	-	-	-	1	-	-	-	-	-	1	-	-	-	-	-	-	-	-	2	99	<i>Alcaligenes faecalis</i> 1C3N	JF710955		
Rare population^a																													
	85	6	2	1	4	2	4	4	1	3	3	1	1	4	2	2	2	4	1	0	4	12	2	8	3	161	Unidentified		
Total clones	88	94	88	88	95	91	94	94	87	95	94	93	91	79	90	93	91	76	96	93	90	74	93	95	93	2255			

^a Rare population included phylotypes which were shown in only one library with less than 2 clones

Supplementary Table S5. Comparison of phylotypes between anolyte solution and anode biofilm under SP operations^a.

Taxonomy Phylotype	SP-H				SP-M				SP-L				% match	Best matched sequence	Accession No.
	a-5		b-5		a-5		b-5		a-5		b-5				
	Anode	Solution	Anode	Solution	Anode	Solution	Anode	Solution	Anode	Solution	Anode	Solution			
<i>Proteobacteria - δ-Proteobacteria</i>															
G11	6	-	4	-	-	1	-	-	-	-	-	-	96	<i>Geobacter</i> sp. strain CdA-2	Y19190
G15	-	-	-	-	19	-	9	-	4	-	-	-	95	<i>Geobacter chapelleii</i>	U41561
MEC_GeoH3	23	-	10	-	-	-	-	-	-	-	-	-	98	<i>Geobacter humireducens</i>	AY187306
MEC_GeoM2	-	-	-	-	7	-	-	-	-	-	-	-	99	<i>Geobacter brementis</i>	JN795198
Geo1	-	-	1	-	2	-	-	-	-	-	-	-	96	<i>Geobacter metallireducens</i> GS-15	CP000148
Su6	-	-	11	-	-	1	-	-	-	-	-	-	99	<i>Geobacter</i> sp. OSK6	AB682759
<i>Proteobacteria - γ-Proteobacteria</i>															
Tol5	3	-	31	3	22	1	19	-	69	70	5	-	99	<i>Tolomonas</i> sp. OCF	GU370947
MEC_TOL2	10	-	-	-	-	-	-	-	1	2	-	-	96	<i>Tolomonas auensis</i> DSM 9187	CP001616
Ma4S_P01	-	-	-	-	-	1	-	-	-	-	-	-	98	<i>Tolomonas auensis</i> DSM 9187	CP001616
Lb4S_D16	-	-	-	-	-	-	-	-	-	12	-	-	99	<i>Tolomonas auensis</i> DSM 9187	CP001616
La4S_K03	-	-	-	-	-	-	-	-	-	-	-	1	99	<i>Tolomonas</i> sp. OCF	GU370947
G13	1	-	-	-	-	-	-	-	-	1	57	5	97	<i>Aeromonas sharmiana</i> GPTSA-6	DQ013306
G12	-	-	-	-	-	-	-	-	-	-	5	3	98	<i>Aeromonas sharmiana</i> CB-8	JF496528
<i>Firmicutes - Bacilli</i>															
G17	33	6	6	15	10	42	25	6	-	-	6	4	100	<i>Lactococcus</i> sp. JXZ-2	JF496551
<i>Firmicutes - Clostridia</i>															
La3_B21	-	-	-	-	-	-	-	-	-	-	-	1	100	<i>Clostridium</i> sp. P2	AY949856
G13	-	-	7	2	1	-	-	-	-	-	3	-	98	<i>Acetobacterium submarinus</i>	AY485791
Ma1_I16	-	-	-	-	-	1	-	-	-	-	-	-	99	<i>Anaerofilum agile</i>	X98011
Mb1_P17	-	-	-	-	-	1	-	-	-	-	-	-	97	<i>Tissierella praeacuta</i> ATCC 33268	GQ461814
Hb1_E17	-	-	-	-	-	-	-	1	-	-	-	-	96	<i>Clostridium</i> sp. NML 04A032	EU815224
<i>Firmicutes - others</i>															
Hb2_E04	-	-	-	-	-	-	-	-	3	1	-	-	92	<i>Phascolarctobacterium</i> m sp. YIT 12068	AB490812
MEC_AV1	6	4	-	-	-	1	28	-	-	-	-	-	99	<i>Anaeroarcus burkinensis</i> DSM 6283	NR_025298
MEC_AV2	1	-	8	1	10	10	-	5	-	-	1	1	98	<i>Anaeroarcus burkinensis</i> DSM 6283	NR_025298
Ma4_P11	-	-	-	-	2	5	-	-	-	-	-	-	99	<i>Anaeroarcus burkinensis</i> DSM 6283	NR_025298
Mb2_F08	-	-	-	-	-	1	-	-	-	-	-	-	92	<i>Veillonellaceae</i> bacterium 6-15	AB603498
<i>Bacteroidetes</i>															
Su2	-	-	4	-	-	-	-	-	3	-	-	-	99	<i>Parabacteroides</i> sp. Lind7H	HQ020488
La3_F03	-	-	-	-	-	-	-	-	-	1	-	-	83	<i>Cytophaga fermentans</i> NBRC 15936	AB517712
G10	1	-	-	-	1	2	2	1	2	1	2	-	85	<i>Bacteroidetes</i> bacterium 4F6B	AB623230
La4_A15	-	-	-	-	-	-	-	1	-	-	4	1	90	<i>Paludibacter propionigenes</i> WB4	CP002345
Ha4S_A11	-	2	-	-	-	-	-	-	-	-	-	-	99	<i>Flavobacterium mizutaii</i> isolate Ch4	AM286271
<i>Other Taxa</i>															
Mb3_K06	-	-	-	-	-	19	-	-	-	-	-	-	99	<i>Alcaligenes faecalis</i> 1C3N	JF710955
Mb3_K08	-	-	-	-	-	-	-	8	-	-	-	-	100	<i>Alcaligenes faecalis</i> AMT-04	AB694009
Ma4S_H13	-	-	-	-	-	3	-	-	-	-	-	-	99	<i>Alcaligenes</i> sp. BJ-23	GQ280033
Ha4S_A03	-	1	-	-	-	-	-	-	-	-	-	-	99	<i>Comamonas</i> sp. P4-4	EU113219
Hb4S_G15	-	-	-	1	-	-	-	-	-	-	-	-	99	<i>Comamonas</i> sp. DF2	KC294053
Ma4S_J07	-	-	-	-	-	1	-	-	-	-	-	-	100	<i>Diaphorobacter oryzae</i> RF21	EU342380
Mb4S_M05	-	-	-	-	-	-	-	1	-	-	-	-	99	<i>Arcobacter cryaerophilus</i> LMG:9865	FR682113
Ma4S_J11	-	-	-	-	-	3	-	-	-	-	-	-	99	<i>Arcobacter cryaerophilus</i> LMG:9865	FR682113
Others ^b	11	-	5	-	17	-	9	-	8	-	10	-			
Total clones	95	13	87	22	91	93	91	23	90	88	93	16			

^a Phylotype comparison was conducted at 5 month samples between anode biofilm (anode) and anolyte solution (sol) after batch.

^b Rare population included phylotypes with less than 2 clones within the anode biofilm.

SUPPLEMENTARY METHODS

Medium composition

The medium for MFC and SP operations contained (per liter) the following: 0.136 g KH_2PO_4 , 1.5 g NH_4Cl , 0.007 g Na_2SO_4 , 0.03 g $\text{MgCl}_2 \cdot 6\text{H}_2\text{O}$, 0.015 g $\text{CaCl}_2 \cdot 2\text{H}_2\text{O}$, 2.52 g NaHCO_3 , 0.01 g Yeast extract, 10 ml vitamin solution (Ishii et al 2005), 1 ml Se/W solution (Ishii et al 2005), and 20 ml trace mineral element solution. The trace mineral element solution contained (per liter) the following: 1350 mg $\text{FeCl}_3 \cdot 6\text{H}_2\text{O}$, 24 mg $\text{CoCl}_2 \cdot 6\text{H}_2\text{O}$, 136 mg ZnCl_2 , 128 mg MnCl_2 , 6.2 mg H_3BO_3 , 37 mg $\text{CuSO}_4 \cdot 5\text{H}_2\text{O}$, 120 mg $\text{NiCl}_2 \cdot 6\text{H}_2\text{O}$, 24.2 mg $\text{Na}_2\text{MoO}_4 \cdot 2\text{H}_2\text{O}$, 47.4 mg $\text{KAl}(\text{SO}_4)_2 \cdot 12\text{H}_2\text{O}$, and 5 drops of concentrated HCl. The medium was anaerobically prepared with N_2/CO_2 (80/20 [vol/vol]) flushing. Four carbon substrates (i.e. 15 mM of acetate for AC-MFCs, mixture of 3.75 mM butyrate and 3.75 mM propionate for BP-MFCs, 5 mM of glucose for GL-MFCs, 2.5 mM of sucrose for SU-MFCs, or 3 mM of sucrose for SP reactors at a final concentration) were anaerobically added to each batch cycle. The concentration of carbon substrates was determined that the substrate was completely consumed by the community around 7 days (Fig. 4 and 5, and Supplementary Fig. S2 and S3). The conductivity of the medium was 3.65 mS/cm, and pH was 7.1, respectively.

HPLC analyses

Volatile fatty acid (VFA) concentrations in the anolyte solution were measured using a high-pressure liquid chromatography (HPLC) machine equipped with a multiple wavelength detector (Agilent 1200 series) and a reverse phase C18 column (Epic Polar, ES Industries or SynergiTM 4 μm Hydro-RP 80 Å, Phenomenex). The eluant was 50 mM phosphoric acid (pH 1.87) for Epic Polar and 0.5 mM sulfuric acid (pH 2.61) for SynergiTM 4 μm Hydro-RP 80 Å at a flow rate of 1.0 ml/min. Acetate, propionate, butyrate, and lactate were identified and determined based on known standards (detection limit was > 0.1 mM).

Scanning electron microscopy (SEM)

A small portion of carbon cloth was collected from the anodes, fixed with 1.25% glutaraldehyde, dehydrated through a series of ethanol dilutions, and dried using a critical point drier (Autosamdri 815, Tousimis) (Gorby et al 2006). The specimens were coated with Pt/Pd and imaged at 2 kV on a LEO 1540XB Field Emission SEM (Carl Zeiss SMT AG).

SUPPLEMENTARY DISCUSSION

Microbial metabolic functions in AC-MFC

Acetate was observed as a substrate or primary fermentation byproduct coupled with electrode respiration (Fig. 4 and 5, and Supplementary Fig. S2 and S3) in all MFC and SP reactors; therefore, the microbial community profile associated with the acetate-fed enrichments is considered a baseline for all other MFC enrichments.

Previous reports have shown that acetate-consuming electrogenic biofilms are typically dominated by family *Geobacteraceae* populations (Kiely et al 2011); however, the microbial community in our AC-MFCs showed three dominant groups, family *Geobacteraceae*, family *Desulfuromonadaceae*, and phylum *Bacteroidetes* (Fig. 7A). The *Desulfuromonas* phylotype Des1 was highly abundant in the early stage of biofilm establishment, while the relative frequency of the *Geobacteraceae* phylotype AC3 increased in the biofilms after a longer enrichment period under MFC operations (Fig. 8). Various strains in family *Desulfuromonadaceae* have been reported as solid iron/electrode reducers with acetate consumption (Roden and Lovley 1993) and have also been observed in electrically active anode biofilms in MFCs (Holmes et al 2004, Ishii et al 2012, Tender et al 2002). This suggests that the dominant *Desulfuromonadaceae* phylotypes Des1 and *Geobacteraceae* phylotype Ac3 were both primary contributors to electricity generation through EET coupled with acetate oxidation; however, the nature of the relationship between these two phylotypes (competitive vs. syntrophic) remains unknown.

Phylum *Bacteroidetes* has been frequently observed in other MFCs fed with acetate (Jung and Regan 2007, Jung and Regan 2011, Zhang et al 2011), suggesting functional traits related to a central metabolism are associated with this phylum. Our AC-MFC biofilms featured two *Bacteroidetes* phylotypes, Ac12 and Ac13, that were highly abundant (Fig. 7A and 8) within the communities; however, those phylotypes were not closely related to other previously reported *Bacteroidetes* strains (Supplementary Fig. S11). This includes *Dysgonomonas oryzae* strain Dy73, which was recently isolated from an MFC and is also capable of MnO₂ reduction (Kodama et al 2012). The general role of the phylum *Bacteroidetes* isolated from the human gut is suggested to be involved in polysaccharide production, uptake, and degradation, and in metabolizing liberated sugars by fermentation (Xu et al 2003). This also suggests the phylotypes Ac12, Ac13, and other less frequent *Bacteroidetes* phylotypes may play a role in the degradation of excess polysaccharide produced by other microbes in the community.

These three taxonomic groups in the AC-MFCs were also observed during the enrichments in other substrate-fed MFCs (Fig. 7A), which also indicates that those microbes played a key role for consuming acetate with EET; however, the dominant phylotypes in the other MFC and SP reactors were not similar to the AC-MFCs (Fig. 8) suggesting that fermentative substrate and electrode surface redox potentials affected to a species or strain selection of acetate-consuming electrode-respiring members.

In addition, the microbial community diversity was lower in the AC-MFC anode biofilms than those fed with more complex substrates like sugars (Supplementary Table S1 and Fig. S6). There was a higher diversity of less frequent phylotypes in the AC-MFCs, especially in phylum

Bacteroidetes and class *Clostridia* at the 3-month operational period (Supplementary Table S3). Those relatively rare populations might also have existed in the sugar-fed MFCs since acetate was also consumed after 1 day of medium exchanges (Fig. 4CD); however, the electrogenic communities in the SU/GL-MFC reactors were highly occupied by *Geobacter* phylotypes and *Tolomonas* phylotypes, which are likely associated with a central metabolism of electrogenic sugar consumption (Fig. 7A and 10A). To address whether rare phylotypes observed in AC-MFCs were also present in the sugar-fed MFCs, we will need to do more sequencing of the 16S rRNA clones from the sugar-consuming communities.

Microbial metabolic functions in BP-MFC

Compared with acetate, butyrate and propionate are less characterized as substrates for the enrichment and evaluation of electrogenic anode biofilms (Chae et al 2009, Freguia et al 2010, Jang et al 2010). The microbial community analyses that have been reported for butyrate- or propionate-fed MFCs have not specifically addressed the taxonomic and functional associations between these carbon sources and electricity generation. Chae *et al.* reported that *Bacilli* were highly represented in a propionate-fed MFC and *Betaproteobacteria* was represented in a butyrate-fed MFC (Chae et al 2009), while Jang *et al.* demonstrated that *Betaproteobacteria* and *Gammaproteobacteria* were observed in a propionate-degrading anode biofilm (Jang et al 2010). However, those groups observed by DGGE did not specifically relate to previously reported propionate-degraders, butyrate-degraders, or electricity generators.

Our BP-MFCs showed that various *Geobacter*-associated phylotypes dominated the electrogenic microbial communities (Fig. 8). Although the phylotype Geo1, closely related to *G. metallireducens* was highly abundant in the communities, other *Geobacter*-associated phylotypes Des1 and Ac3 were also observed (Fig. 9A). This result suggests that different types of electrogenic *Geobacter* strains were necessary to consume the mixture of propionate, butyrate, and acetate in the BP-MFCs.

In addition, the BP-MFC enriched *Clostridia*-associated phylotypes BP20 (closely related to those of the genus *Syntrophomonas*), and Ac5 (closely related to *Acetoanaerobium noterae*) (Fig. 7A and Supplementary Fig. S10). The family *Syntrophomonadaceae* is known to include butyrate oxidizers (Muller et al 2010), suggesting that the phylotype BP20 contributed to butyrate degradation in the electrogenic communities. *Acetoanaerobium noterae* has been previously characterized as an acetogenic bacterium which converts H₂ and CO₂ to acetate (Sleat et al 1985), suggesting that the phylotype Ac5 is associated with acetate-related metabolism in the biofilm. The results collected from our BP-MFCs yield more convincing data than previously reported for butyrate degradation and electricity generation (Chae et al 2009, Freguia et al 2010, Jang et al 2010), and addresses how the microbial community metabolizes these VFAs and generates electricity. As for propionate degradation, there is no evidence of direct electricity generation with propionate consumption, and no potential propionate degrader has yet been observed in propionate-fed MFCs (Chae et al 2009, Freguia et al 2010, Jang et al 2010). Our results also revealed no clear image of propionate-consuming electricity generation. The possibility also exists that the *Syntrophomonas* and *Acetoanaerobium* phylotypes may syntrophically cooperate with *Geobacter* phylotype Geo1 (dominant only in the BP-MFCs) enabling effective EET reactions from butyrate and propionate (Fig. 10A).

Sugar metabolism-related strains in EET-active communities

Phylotypes only observed in the sugar-fed MFC and SP reactors are considered as key microbes related to sugar fermentation within the electrogenic microbial communities. We found that two *Gammaproteobacteria* phylotypes Tol1 and Tol9, classified to family *Aeromonadaceae* and genus *Tolomonas* (Fig. 9B), increased in population frequency throughout the MFC enrichment process only in the GL/SU-MFCs (Fig. 8). In addition, we found one *Gammaproteobacteria* phylotype Tol5, also classified to family *Aeromonadaceae* and genus *Tolomonas*, had significantly high relative abundance within all SP reactors (Fig. 8). These trends strongly suggest that the *Tolomonas*-associated phylotypes play an important role for sugar fermentation and supply critical VFAs that can be consumed in subsequent reactions (Fig. 3CD, 5, and 10A). Two *Tolomonas* isolates have been described in the literature as fermentative microbes including strain TA 4^T and OCF7 (Caldwell et al 2011, Fischer-Romero et al 1996), while one electrochemically active *Tolomonas* strain P2-A-1 has recently been isolated from MFC (Luo et al 2013). The family *Aeromonadaceae* includes a couple of *Aeromonas* strains that have been isolated from MFCs such as *Aeromonas hydrophila* (Pham et al 2003) and *Aeromonas* sp. strain ISO2-3 (Chung and Okabe 2009a), which were reported as electricity-generating bacteria using glucose and hydrogen as energy sources (Chung and Okabe 2009b, Pham et al 2003). These features suggest that the *Tolomonas*-associated phylotypes in our MFC and SP reactors functioned mainly as the dominant fermentor in the anodic microbial communities. However, the possibility exists that the *Tolomonas* phylotypes were so abundant because they were directly involved with electrode reduction and/or may have syntrophic cooperation with specific *Geobacter* phylotypes observed in each reactor. The involvement in EET reactions (directly or indirectly) of the *Tolomonas* microbes might explain their high frequency in the enriched electrogenic biofilms fed with sugar compounds under lower EET rate conditions (GL/SU-MFC and SP-L reactors). This finding is new relative to other reports that have frequently described *Clostridia*, *Bacilli*, or *Bacteroidetes* as fermenters in the other glucose-fed MFCs (Jung and Regan 2007, Jung and Regan 2011, Xing et al 2009, Zhang et al 2011).

Instead of *Tolomonas*-associated phylotypes, we found a relatively high frequency of two *Firmicutes* phylotypes, *Lactococcus* phylotype G117 and *Anaeroarcus* phylotype G118, in the enriched electrogenic biofilms and anolyte solutions under higher EET rate conditions in the SP-H/M reactors (Fig. 8). Genus *Lactococcus* is a well-known group of lactic acid bacteria that produces lactic acid as the major or only product of glucose fermentation (Bolotin et al 2001). The metabolic trends of SP-H/M reactors at 5 months of operation showed lactate production coupled to initial sucrose fermentation happening within 10 hours after medium exchange (Fig. 5BD and Supplementary Fig. S3BD), which also suggests that lactic acid bacteria were actively working in the SP-H/M reactors (Fig. 10A). Genus *Anaeroarcus* is reported as an obligately anaerobic chemo-organotroph that can ferment a limited range of organic acids, amino acids, carbohydrates and alcohols, which are converted to mainly acetate, propionate, succinate and propanol (Strompl et al 1999). Fig. 10B suggests that genus *Anaeroarcus* was related to maximum current density in SP-H/M reactors. *Anaeroarcus burkinensis* DSM 6283, which is most closely related to the phylotype G118, has been reported to reduce soluble ferric iron coupled with lactate consumption to make acetate (Ouattara et al 1992). This suggests the possibility that the phylotype G118 might facilitate EET reactions using its soluble iron-reducing machinery.

***Geobacter* phylotype trends in EET-active communities**

Fig. 7B and 8 showed dynamics of *Geobacter*-affiliated phylotypes under SP conditions with different anode electrode potentials. The results indicate that more positive electrode potentials (SP-H/M reactors) resulted in higher current production and higher abundance of *Geobacter* spp. relative to the electronegative electrode potentials (SP-L reactor). The exceptions to this trend were SP-M-b2 that did not show *Geobacter* phylotypes, and SP-L-b3 that had a high abundance of *Geobacter* phylotypes.

Even with ~25 mA of operational current in the SP-M-b2 reactor (Fig. 2B), *Geobacter*-affiliated phylotypes were not observed in the anode microbial community (Fig. 7B). It is postulated that the SP-M-b2 community was in a transition phase of dominant *Geobacter* phylotypes from phylotypes Geo2 and G11, to phylotypes Ac3 and G115 (Fig. 8). During this transition phase, it is possible that the *Geobacter* portion in the community might be reduced. Additionally, the SP-M-b2 community showed a rapid and significant increase of overall biofilm biomass density (Fig. 6B) including a considerable increase in the relative frequency of the fermentative microbes, *Lactococcus* phylotype G117 and *Anaerococcus* phylotype G118 (Fig. 7B and 8). These phenomena suggest that the EET-active *Geobacter* phylotypes were present in such a low abundance within the community that the clone library method for the SP-M-b2 sample (90 clones sequenced) was not sufficient for detecting the genera. Fermentor microbes were also dominant in the anode biofilm at the time, further decreasing the chance of detecting *Geobacter* spp.

The SP-L-b reactor showed relatively slow performance trends with respect to establishing current generation (Fig. 2C), which suggests that the community development was also slow compared to the other three sucrose-fed MFC/SP reactors. The *Geobacter* phylotype G11 was highly dominant at the 3-month operation of the SP-L-b reactor and this trend was not observed for the other low current-generating reactors (SP-L-a and SU-MFCs). However, the phylotype G11 was found to be present within a group of three *Geobacter* phylotypes (Geo1, G11, and G12) that were frequently observed at the early stages of community development in SP-L-a and SU-MFCs (Fig. 8). These phenomena suggest that the high abundance of *Geobacter* phylotypes in SP-L-b2 reactor was related to an initial activation of *Geobacter* growth frequently observed at earlier stage in the other reactors.

One of the preceding reports (Torres et al 2009) concluded the opposite trends for electrode potential preferences of *Geobacter* spp. Torres et al. found that a positive anode potential (+370 mV vs SHE) under SP conditions resulted in a lower abundance of *Geobacter* phylotypes and very low current generation relative to electronegative anode potentials. The *Geobacter* phylotypes were reported as relating to *Geobacter sulfurreducens*, which is a member of the *G. metallireducens* clade (Torres et al 2009). In our SP-H/M reactors (+100 mV or -50 mV vs. SHE, respectively), the phylotypes affiliated to the *G. metallireducens* clade (Fig. 9A) were not abundantly observed (Fig. 8). Instead, our SP-H/M reactors showed a high relative abundance of phylotypes affiliated to *Geobacter* Subsurface clades 1 and 2, which are hypothesized to be electricity generators that are well adapted to more electropositive anode potentials (Fig. 10B). It is possible that members of the *Geobacter* Subsurface clades 1 and 2, as well as genus *Desulfuromonas*, were not inoculated in the previous report (Torres et al 2009), since their inoculum source was wastewater and not sediment. Additionally, we did not operate our reactors at such high electropositive potentials. The Torres et al. report found higher abundances of *Geobacter* phylotypes associated with the +200 mV, -90 mV and -150 mV (vs. SHE) operational potentials, which is generally in agreement with our findings. However, as

noted above, the phylogenetic differences found at the more electronegative potentials in our study, relative to the Torres et al. report, is likely due to the inoculum sources.

SUPPLEMENTARY REFERENCES

Bolotin A, Wincker P, Mauger S, Jaillon O, Malarne K, Weissenbach J *et al* (2001). The complete genome sequence of the lactic acid bacterium *Lactococcus lactis* ssp. *lactis* IL1403. *Genome Res* **11**: 731-753.

Caldwell ME, Allen TD, Lawson PA, Tanner RS (2011). *Tolumonas osonensis* sp. nov., isolated from anoxic freshwater sediment, and emended description of the genus *Tolumonas*. *Int J Syst Evol Microbiol* **61**: 2659-2663.

Chae KJ, Choi MJ, Lee JW, Kim KY, Kim IS (2009). Effect of different substrates on the performance, bacterial diversity, and bacterial viability in microbial fuel cells. *Bioresour Technol* **100**: 3518-3525.

Chung K, Okabe S (2009a). Continuous power generation and microbial community structure of the anode biofilms in a three-stage microbial fuel cell system. *Appl Microbiol Biotechnol* **83**: 965-977.

Chung K, Okabe S (2009b). Characterization of electrochemical activity of a strain ISO2-3 phylogenetically related to *Aeromonas* sp. isolated from a glucose-fed microbial fuel cell. *Biotechnol Bioeng* **104**: 901-910.

Fischer-Romero C, Tindall BJ, Juttner F (1996). *Tolumonas auensis* gen. nov., sp. nov., a toluene-producing bacterium from anoxic sediments of a freshwater lake. *Int J Syst Bacteriol* **46**: 183-188.

Freguia S, Teh EH, Boon N, Leung KM, Keller J, Rabaey K (2010). Microbial fuel cells operating on mixed fatty acids. *Bioresour Technol* **101**: 1233-1238.

Gorby YA, Yanina S, McLean JS, Rosso KM, Moyles D, Dohnalkova A *et al* (2006). Electrically conductive bacterial nanowires produced by *Shewanella oneidensis* strain MR-1 and other microorganisms. *Proc Natl Acad Sci U S A* **103**: 11358-11363.

Holmes DE, Bond DR, O'Neil RA, Reimers CE, Tender LR, Lovley DR (2004). Microbial communities associated with electrodes harvesting electricity from a variety of aquatic sediments. *Microb Ecol* **48**: 178-190.

Ishii S, Kosaka T, Hori K, Hotta Y, Watanabe K (2005). Coaggregation facilitates interspecies hydrogen transfer between *Pelotomaculum thermopropionicum* and *Methanothermobacter thermautotrophicus*. *Appl Environ Microb* **71**: 7838-7845.

- Ishii S, Suzuki S, Norden-Krichmar TM, Nealsen KH, Sekiguchi Y, Gorby YA *et al* (2012). Functionally stable and phylogenetically diverse microbial enrichments from microbial fuel cells during wastewater treatment. *PLoS One* **7**: e30495.
- Jang JK, Chang IS, Hwang HY, Choo YF, Lee J, Cho KS *et al* (2010). Electricity generation coupled to oxidation of propionate in a microbial fuel cell. *Biotechnol Lett* **32**: 79-85.
- Jung S, Regan JM (2007). Comparison of anode bacterial communities and performance in microbial fuel cells with different electron donors. *Appl Microbiol Biotechnol* **77**: 393-402.
- Jung S, Regan JM (2011). Influence of external resistance on electrogenesis, methanogenesis, and anode prokaryotic communities in microbial fuel cells. *Appl Environ Microbiol* **77**: 564-571.
- Kiely PD, Regan JM, Logan BE (2011). The electric picnic: synergistic requirements for exoelectrogenic microbial communities. *Curr Opin Biotechnol* **22**: 378-385.
- Kodama Y, Shimoyama T, Watanabe K (2012). *Dysgonomonas oryzaevi* sp. nov., isolated from a microbial fuel cell. *Int J Syst Evol Microbiol*. **62**: 3055-9
- Luo J, Yang J, He H, Jin T, Zhou L, Wang M, Zhou M (2013). A new electrochemically active bacterium phylogenetically related to *Tolomonas osonensis* and power performance in MFCs. *Bioresour Technol* **139**: 141-148.
- Muller N, Worm P, Schink B, Stams AJM, Plugge CM (2010). Syntrophic butyrate and propionate oxidation processes: from genomes to reaction mechanisms. *Env Microbiol Rep* **2**: 489-499.
- Ouattara AS, Traore AS, Garcia JL (1992). Characterization of *Anaerovibrio-Burkinabensis* sp-nov, a lactate-fermenting bacterium isolated from rice field soils. *Int J System Bacteriol* **42**: 390-397.
- Pham CA, Jung SJ, Phung NT, Lee J, Chang IS, Kim BH *et al* (2003). A novel electrochemically active and Fe(III)-reducing bacterium phylogenetically related to *Aeromonas hydrophila*, isolated from a microbial fuel cell. *FEMS Microbiol Lett* **223**: 129-134.
- Roden EE, Lovley DR (1993). Dissimilatory Fe(III) reduction by the marine microorganism *Desulfuromonas acetoxidans*. *Appl Environ Microbiol* **59**: 734-742.
- Sleat R, Mah RA, Robinson R (1985). *Acetoanaerobium noterae* gen. nov., sp. nov.: an anaerobic bacterium that forms acetate from H₂ and CO₂. *Int J Syst Bacteriol* **35**: 10-15.
- Strompl C, Tindall BJ, Jarvis GN, Lunsdorf H, Moore ER, Hippe H (1999). A re-evaluation of the taxonomy of the genus *Anaerovibrio*, with the reclassification of *Anaerovibrio glycerini* as *Anaerosinus glycerini* gen. nov., comb. nov., and *Anaerovibrio burkinabensis* as *Anaeroarcus burkinensis* [corrig.] gen. nov., comb. nov. *Int J Syst Bacteriol* **49 Pt 4**: 1861-1872.
- Tender LM, Reimers CE, Stecher HA, Holmes DE, Bond DR, Lowy DA *et al* (2002). Harnessing microbially generated power on the seafloor. *Nat Biotechnol* **20**: 821-825.

Torres CI, Krajmalnik-Brown R, Parameswaran P, Marcus AK, Wanger G, Gorby YA *et al* (2009). Selecting anode-respiring bacteria based on anode potential: phylogenetic, electrochemical, and microscopic characterization. *Environ Sci Technol* **43**: 9519-9524.

Xing D, Cheng S, Regan JM, Logan BE (2009). Change in microbial communities in acetate- and glucose-fed microbial fuel cells in the presence of light. *Biosens Bioelectron* **25**: 105-111.

Xu J, Bjursell MK, Himrod J, Deng S, Carmichael LK, Chiang HC *et al* (2003). A genomic view of the human-*Bacteroides thetaiotaomicron* symbiosis. *Science* **299**: 2074-2076.

Zhang Y, Min B, Huang L, Angelidaki I (2011). Electricity generation and microbial community response to substrate changes in microbial fuel cell. *Bioresour Technol* **102**: 1166-1173.